Dynamical approach to anomalous diffusion: Response of Lévy processes to a perturbation

György Trefán,[1] Elena Floriani,[2] Bruce J. West,[1] and Paolo Grigolini[1,2,3]
[1]*Department of Physics of the University of North Texas, P.O. Box 5368, Denton, Texas 76203*
[2]*Dipartimento di Fisica dell'Università di Pisa, Piazza Torricelli 2, 56100 Pisa, Italy*
[3]*Istituto di Biofisica del Consiglio Nazionale delle Ricerche, Via San Lorenzo 26, 56127 Pisa, Italy*
(Received 28 April 1994)

Lévy statistics are derived from a dynamical system, which can be either Hamiltonian or not, using a master equation approach. We compare these predictions to the random walk approach recently developed by Zumofen and Klafter for both the nonstationary [Phys. Rev. E **47**, 851 (1993)] and stationary [Physica A **196**, 102 (1993)] case. We study the unperturbed dynamics of the system analytically and numerically and evaluate the time evolution of the second moment of the probability distribution. We also study the response of the dynamical system undergoing anomalous diffusion to an external perturbation and show that if the slow regression to equilibrium of the variable "velocity" is triggered by the perturbation, the process of diffusion of the "space" variable takes place under nonstationary conditions and a conductivity steadily increasing with time is generated in the early part of the response process. In the regime of extremely long times the conductivity becomes constant with a value, though, that does not correspond to the prescriptions of the ordinary Green-Kubo treatments.

PACS number(s): 05.40.+j, 05.45.+b, 05.60.+w, 47.27.Qb

I. INTRODUCTION

The foundations of our understanding of statistical physics are the phenomenological theory of Brownian motion and stochastic processes [1] together with the chaotic behavior of nonintegrable Hamiltonian systems [2]. The latter motion is an intrinsic property of nonlinear dynamical systems [3], whereas the former motion results from the system of interest being coupled to the environment. If a dynamical system such as the standard map is fully chaotic, meaning that all the KAM (Kolmogorov-Arnold-Moser) tori have dissolved into a chaotic sea, then the average energy of the system increases linearly with time and the system is diffusive. This connection between statistics and dynamics has been known for nearly two decades [4], but it is only recently that this connection has been systematically exploited to provide a dynamical basis for statistical physics [5].

Concurrently, explaining the phenomenon of anomalous diffusion in which the mean square amplitude of a process increases in time as t^{2H} with $H \neq \frac{1}{2}$ has attracted the attention of a number of investigators. This phenomenon is found in the phase diffusion in the chaotic regime of a Josephson junction [6], chaos-induced turbulent diffusion [7], the relationship between the rms characteristic length of a polymer and the number of monomer units [8], diffusion of a Brownian particle in pure shear flow [9], the zero-component spin model with long-range interaction [10], and the diffusion of a passive scalar in a turbulent flow field [11]. The description of such processes using nondiffusive Lévy statistics has been popular among a number of researchers [12–14]. Scientists are now searching to make the proper connection between Lévy stable processes and certain dynamical systems. The key element is *weak chaos,* in which stable islands persist in the chaotic sea. A number of investigators maintain that this coexistence of stable islands, cantori, and the chaotic sea produces Lévy statistics due to the chaotic orbit sticking to the cantori at the phase space boundary between the two types of motion [15–21]. The results obtained by Zumofen and Klafter [15] within the framework of the continuous-time random walks (CTRW's) are of particular interest. They used two approaches, the jump model (JM), in which the particles wait at a certain location, then jump instantaneously between sites, and the velocity model (VM), where particles move at a constant velocity between turning points, where they choose a new direction at random. Remarkably, the two models result in the same Lévy distribution. The CTRW method has been more recently applied [22] to the case where the dynamical process is the standard map. It is remarkable that Ishizaki *et al.* [20] independently derived the Lévy distribution for a histogram of chaotic trajectories generated by the standard map.

From a dynamical point of view, all diffusion processes, anomalous as well as normal, result from the integration of the equation of motion

$$\dot{x}(t)=\xi \ , \tag{1.1}$$

where ξ is a statistical variable characterized by the equilibrium autocorrelation function

$$\Phi_\xi(t)\equiv\frac{\langle \xi(0)\xi(t)\rangle}{\langle \xi^2\rangle} \ . \tag{1.2}$$

Under the stationarity assumption, it can be shown [23] that

$$\langle x^2(t)\rangle=\langle x^2(0)\rangle+2\langle \xi^2\rangle_{\rm eq}\int_0^t dt'\int_0^{t'} dt''\Phi_\xi(t'') \ . \tag{1.3}$$

The dynamical process under study in this paper rests on the dynamical variable ξ virtually fluctuating among two

distinct values, 1 and -1, with the form of the waiting time distribution $\psi(t)$ in each of these two states. Under this specific condition [6(a)] the expression for the correlation function $\Phi_\xi(t)$

$$\Phi_\xi(t)=\frac{1}{\langle \xi^2 \rangle}\frac{1}{\langle t \rangle}\int_t^\infty dt'(t'-t)\psi(t') \tag{1.4}$$

is derived. Here $\langle t \rangle$ is the mean waiting time in one of the two states of the variable ξ,

$$\langle t \rangle \equiv \int_0^\infty t\psi(t)dt \ . \tag{1.5}$$

Equation (1.3) is exact and when it is supplemented by (1.4) it provides a reliable expression for the second moment. This equation rests on the stationary condition, namely, the state where the distribution of the variable ξ is time independent. Ordinary diffusion is obtained under the condition that the variable ξ is characterized by a finite time scale, defined by

$$\tau \equiv \int_0^\infty dt\, \Phi_\xi(t) \ . \tag{1.6}$$

Ordinary diffusion is exhibited at times much larger than this time scale, where the stationary condition is naturally realized for whatsoever initial conditions are considered. In this case, the two time scales $\langle t \rangle$ and τ have the same order of magnitude. Anomalous diffusion, on the other hand, is generated when the correlation function $\Phi_\xi(t)$ in the long-time limit has an inverse power-law behavior,

$$\lim_{t\to\infty}\Phi_\xi(t)\approx\pm\frac{k}{t^\beta} \ . \tag{1.7}$$

The focus of this paper is on Lévy processes, and hence those which evolve faster than standard diffusion. This implies [23] that (1.7) has positive tails and

$$0<\beta<1 \ . \tag{1.8}$$

This means that in this case the only characteristic time scale left is $\langle t \rangle$, since the correlation time τ diverges.

In this specific condition the correlation function of the variable ξ is remarkably slow, and also the process of regression to equilibrium of its distribution is remarkably slow. For this reason anomalous diffusion is strongly affected by the initial condition considered. If the variable velocity ξ is given an initial condition not corresponding to the equilibrium state, it gradually evolves towards its equilibrium and it strongly influences the diffusion process of the variable x. Zumofen and Klafter have explored both the nonstationary condition for the JM and VM [15,17], and the stationary condition for the VM [16,17], and have pointed out the remarkable differences exhibited by the diffusion process under these two different conditions.

The focus of the present paper is on the response of anomalous diffusion to external perturbations. However, before addressing this issue, we provide the reader with a clear perspective of the way a dynamical equation of motion such as (1.1) leads to Lévy statistics, as a relevant example of nonordinary statistical mechanics. To do this we adopt a master equation (ME) approach. In principle, the ME approach plays a major role in the rigorous derivation of a transport process from a Liouville equation [24(b)]. This is so because the ME in either the normal [25] or generalized [26] form has a structure which can be formally derived from the Liouville equation by means of a projection method [24]. This is the route followed by Bianucci *et al.* [5] to derive ordinary statistical mechanics from a fully chaotic dynamical process. The microscopic origin of anomalous diffusion implies a departure from this ideal condition, thereby making harder the adoption of the projection method as a theoretical tool to derive diffusion from a process of deterministic dynamics. The present paper is less ambitious and the ME approach rests essentially on intuitive arguments and the suggestions provided by the work of Seshadri and West [27] rather than on a microscopic derivation. However, this approach makes transparent the derivation of Lévy processes from a dynamical picture.

Let us illustrate the basic idea used to derive the Lévy distribution on the basis of intuitive ME arguments. A stationary Lévy process is characterized by the following distinctive property. The Fourier-Laplace transform of the Lévy distribution $P(x,t)$, denoted by $\hat{P}(k,s)$, has the explicit form

$$\hat{P}(k,s)=\frac{1}{s+b|k|^\alpha} \ , \tag{1.9}$$

with

$$0\le\alpha\le 2 \ . \tag{1.10}$$

Seshadri and West [27] noticed that the probability distribution $P(x,t)$ obeys the following equation of motion:

$$\frac{\partial}{\partial t}P(x,t)=b\frac{1}{\pi}\sin\left[\frac{\pi\alpha}{2}\right]\Gamma(1+\alpha) \otimes\int_{-\infty}^{\infty}dy\frac{1}{|x-y|^{1+\alpha}}P(y,t) \ . \tag{1.11}$$

This equation is not a ME, because the population at a given site with coordinate x can only change because of the transitions from other sites y. In a proper ME the population at the given site x should also undergo a decay process due to transitions away from this site to all the other sites in the available space. However, (1.11) suggests that a Lévy process might be generated within a ME approach by transitions from a site y to a site x with probability proportional to $1/|x-y|^{\alpha+1}$. To make this clear consider a realization of this kind of ME on an infinite lattice, whose coordinates are the discrete variables

$$x_r=\Delta r \ , \tag{1.12}$$

with

$$r=\pm1,\pm2,\ldots \ , \tag{1.13}$$

and Δ the constant lattice spacing. The ME can be written

$$\frac{\partial}{\partial t}P(r,t)=-\Gamma_r P(r,t)+\sum_{r'}A_{r',r}P(r',t) \ , \tag{1.14}$$

with a positive definite decay constant

$$\Gamma_r = \sum_{r'} A_{r,r'} \ . \tag{1.15}$$

Let us now assume that the transition matrix has elements

$$A_{r,r'} = \frac{\kappa}{|r\Delta - r'\Delta|^{\alpha+1}} \ . \tag{1.16}$$

The second term on the right-hand side (rhs) of (1.14) can be divided into two parts: the first refers to the r''s satisfying the condition $|r-r'| < n_T$, and the second to the r''s with $|r-r'| \geq n_T$. Note that n_T is a positive integer, and that if it is large enough the second contribution can be replaced by an integration over the continuous variable y. The long-time dynamics of this system essentially depends on this second term. On the other hand, if we neglect the contribution of $|r-r'| < n_T$ to the sum in (1.14) as well as the first term on the rhs of (1.14), the remaining contribution leads to dynamics indistinguishable from that described by (1.11). This is how a ME can lead in the asymptotic time region to a behavior indistinguishable from that of a Lévy process.

In Sec. II we shall show that the ME enables us to establish the correct asymptotic properties of the correlation function $\Phi_\xi(t)$, the second moment $\langle x^2(t) \rangle$, and the probability distribution $P(x,t)$, in complete accord with the recent findings of Mori and co-workers [2,20]. According to the projection method [24] the ME, with no inhomogeneous term, refers to the stationary condition [24]. Although (1.4) is not exact, it is expected to be correct if we can neglect the fluctuations making $|\xi|$ depart slightly from 1. The ME rests on the same approximation, but it does not lead to the same result, albeit the power of the resulting inverse power law for $\Phi_\xi(t)$ is the same. This is where the ME needs further improvements to share the nice property of the stationary VM, which is found to be in full agreement with (1.3) supplemented by (1.4).

The central result of this paper concerns the response of anomalous diffusion, in the Lévy regime, to external perturbations. According to the standard Green-Kubo method [28] the response of a normal diffusion process to a perturbation resulting in a bias should be given by

$$\frac{d}{dt}\langle x(t) \rangle = K \int_0^t \langle \xi(0)\xi(t') \rangle_{\rm eq} dt' \ , \tag{1.17}$$

where K is a constant depending on the physical details of the system considered. If we imagine (1.17) to be applicable also to the case of anomalous diffusion, we are led to conclude that a stationary current, namely, a constant velocity $\langle \dot{x} \rangle$, is not allowed. The power-law dependence (1.7) with the condition (1.8) suggests that in the case of anomalous diffusion conductivity might become time dependent and increase as a function of time. We shall prove that this property applies to the early stage of the response subsequent to an abrupt perturbation, and that in the long-time regime a finite conductivity is recovered, albeit with a value not corresponding to the standard Green-Kubo prescriptions.

The outline of the paper is as follows. Section II is devoted to illustrating the ME arguments. Section III describes the dynamical model to which our theoretical arguments and numerical calculations are applied. The most relevant aspects of the numerical technique here adopted are described. The unperturbed dynamical evolution of this model is studied in Sec. IV, where we compare the theoretical prediction of the ME approach on the time evolution of the second moment $\langle x^2(t) \rangle$ to both the stationary and nonstationary predictions of Zumofen and Klafter [15–17] and to the corresponding results of numerical "experiments." In Sec. V we study the response of the dynamical system to a geometrical and a dynamical perturbation both analytically and numerically. In the dynamical perturbation case, with the help of the stationary and nonstationary versions of the VM, and with the support of numerical calculations, we illustrate the transition from the early process of anomalous response, with a time-dependent conductivity, to the long-time regime of "normal" response, with a time-independent conductivity. Concluding remarks on the results of this paper are made in Sec. VI.

II. THE ME APPROACH

The question of the equivalence of the ME and certain random walks, raised by Bedeaux, Lakatos-Lindenberg, and Shuler [25], was satisfactorily solved by Kenkre, Montroll, and Shlesinger [26] by establishing a connection between a random walk and a generalized ME of the following structure:

$$\frac{\partial}{\partial t} P(x,t) = \int_0^t dt' \int_{-\infty}^{\infty} dx' K(x-x', t-t') P(x',t') \ , \tag{2.1}$$

where the kernel $K(x,t)$ has the following detailed balance structure:

$$K(x,t) = \Pi(x,t) - \delta(x) \int_{-\infty}^{\infty} \Pi(x',t) dx' \ . \tag{2.2}$$

The approach developed herein, essentially valid only for the dynamical derivation of Lévy processes, does not depend on any random walk theory, and directly derives the structure of $\Pi(x,t)$ using physical arguments to establish the equivalence between (2.1) and (1.11).

The dynamical approach to Lévy processes followed in this paper is based on a map studied for the same purpose by Zumofen and Klafter (see Sec. III). This map describes the motion of the velocity ξ, which is a variable randomly fluctuating between the two possible values, -1 and 1. This makes it possible for the variable velocity ξ to stay in one of these two states with the waiting time distribution

$$\psi(t) = \frac{A}{(B+t)^\mu} \ . \tag{2.3}$$

Normalization requires $\mu > 1$; the normalization condition also sets

$$A = (\mu - 1) B^{\mu-1} \ . \tag{2.4}$$

From the theory of [15] we obtain (see also Secs. III and V)

$$B=\frac{\mu-1}{2} . \tag{2.5}$$

On the one hand, from the time integration of (1.1) we immediately see that anomalous diffusion must be a consequence of a lack of time scale for the variable ξ and, consequently, of the non-Markovian properties ineluctably associated with this lack of a time scale. On the other hand, a Lévy process is the exact solution of the Bachelier-Smoluchowsky-Chapman-Kolmogorov equation [12] and is essentially a Markov process. We show that it is possible to make these two seemingly quite different processes compatible if we make the non-Markovian properties stemming from the inverse power-law behavior of the velocity autocorrelation function become transition probabilities with an inverse power-law dependence on the length of the jump in space [14]. Consequently, we change the time nonlocality into a space nonlocality, and we show that the latter is the space nonlocality of the Lévy processes expressed by (1.11). This space nonlocality cannot be eliminated by observing suitably large distances because of the inverse power-law structure of the corresponding space transition.

The connection between nonlocality in space and nonlocality in time is established by remarking that, throughout the whole period of time t spent by the particle within one of its two velocity states, the particle makes a jump of length $|x|=t$. This means that the probability of making a jump from one site to another at a distance $|x|$ from the initial site is proportional to the waiting time distribution, namely,

$$M(x)\propto\int_0^\infty \Pi(x;t)dt \propto \frac{A}{(B+|x|)^\mu} . \tag{2.6}$$

Thus the connection with the structure of (1.11) and (1.16) is established, provided that we set

$$\mu=1+\alpha . \tag{2.7}$$

However, it is still necessary to determine how the Markovian character underlying the Lévy processes is recovered from the ME. Lévy processes are rigorously Markovian [12], whereas the generalized master equation (2.1) was originally constructed [26] for the purpose of reproducing the predictions of the random walk theories at any time scale, and for this reason has been made explicitly non-Markovian. Actually, the dependence of $\Pi(x,t)$ on time, in principle, cannot be neglected because the transition beginning at one site and ending at another a distance $|x|$ away takes a time $t=|x|$ to occur. Thus the following condition must be fulfilled:

$$\Pi(x,t)\propto\psi(x,t) , \tag{2.8}$$

where $\psi(x,t)$ is the probability distribution introduced by Zumofen and Klafter [15] to move a distance x in a time t in a single motion event. This transition probability reads

$$\psi(x,t)=\tfrac{1}{2}\delta(|x|-t)\psi(t) . \tag{2.9}$$

In conclusion, the motion of x must be non-Markovian. This is a consequence of the fact that the statistical and dynamical properties of x are determined by other variables, namely, ξ and, if necessary, the set of variables required to describe the motion of ξ. As pointed out in [24(a)], the non-Markovian properties of a variable of interest are a necessary consequence of a picture where the dynamics of these additional variables is not explicitly taken into account. Thus, the Lévy processes can only be an idealization of the long-time limit, and if the long-time limit is compatible or not with the Markovian assumption is indeed a condition to assess for the dynamical derivation of these processes.

It must be remarked that the time rate of change of $P(x,t)$ is obtained by integration over space and time of $\Pi(x,t)$. This implies that the proportionality constant in (2.8) has the dimensions of an inverse time, so that

$$\Pi(x,t)=\frac{1}{T}\psi(x,t) . \tag{2.10}$$

Since, as pointed out in Sec. I, the only time scale available in the region $2<\mu<3$ is the mean waiting time $\langle t\rangle$, Eq. (1.5), we are naturally led to identify T with it,

$$T=\langle t\rangle=\frac{B}{\mu-2} . \tag{2.11}$$

In Appendix A we support this choice of time scale with arguments derived by the random walk theory [29].

Let us now consider the Laplace-Fourier transform of (2.1):

$$\hat{P}(k,s)=\frac{1}{s-\hat{K}(k,s)} . \tag{2.12}$$

We adopt the convention that $\hat{F}(k,s)$ denotes the Fourier-Laplace transform of the function $F(x,t)$ and $\hat{G}(s)$ the Laplace transform of the function $G(t)$. By using the expressions for the kernel (2.2) and (2.10) we obtain for $\hat{K}(k,s)$ the following explicit form:

$$\hat{K}(k,s)=\frac{\hat{\psi}(k,s)-\hat{\psi}(s)}{T} , \tag{2.13}$$

where, according to our conventions, $\hat{\psi}(k,s)$ is the Laplace-Fourier transform of (2.9) and $\hat{\psi}(s)$ is the Laplace transform of the waiting time distribution $\psi(t)$.

To derive the Lévy distribution only one basic step remains: we have to properly implement the Markovian approximation in (2.13). This means that we have to look for the limiting value of $\hat{K}(k,s)$ in the large-space, long-time limit where $k\to 0$ and $s\to 0$ together. If the outcome of this asymptotic procedure is to be a Lévy process, which is characterized by the rescaling property [12]

$$x\approx t^{1/\alpha} , \tag{2.14}$$

then it is convenient to set

$$s\approx k^\alpha . \tag{2.15}$$

Using the rescaling property (2.15) and the condition $\alpha>1$, which implies s tending to zero faster than k, we obtain [note that α is related to μ by (2.7)]

$$\hat{P}(k,s)=\frac{1}{s+b|k|^\alpha} , \tag{2.16}$$

with

$$b=\frac{B^{\mu-1}\Gamma(2-\mu)}{T}\cos\left[\frac{\pi}{2}(\mu-1)\right] . \tag{2.17}$$

It is worthwhile to notice that this prediction coincides with that of the JM and VM in both the stationary and nonstationary regimes. The JM in the stationary regime has not been explicitly dealt with by Zumofen and Klafter [16,17]. Thus, in Appendix B we illustrate the theoretical arguments necessary to derive the probability distribution for the JM in this case. Details on the calculation leading to (2.17) and to proving the coincidence between this prediction and those of the VM and JM theories, in both the stationary and nonstationary regimes, are given in Appendix C.

It must be remarked that the theory developed in this section is tailored to the region $2<\mu<3$. The region with $\mu<2$ ($\alpha<1$) is excluded by the fact that for $\mu<2$ the first moment of the waiting time distribution diverges, thereby preventing us from defining the time scale $T=\langle t\rangle$. Furthermore, even if T were arbitrarily given a finite value, and α were still identified with $\mu-1$ [see (2.7)] in the asymptotic limit of vanishing k and s the resulting value of b would vanish. The region $\mu>3$ is excluded by the fact that the Markovian approximation leads to the structure (2.16) with $\alpha>2$, in which case $P(x,t)$ is not positive definite [12].

At this stage it is worthwhile to show that the theoretical and numerical results obtained by Mori and coworkers in their investigation of accelerated modes of the standard map [20] adhere to the prescriptions of the above theory. In that case the asymptotic waiting time distribution is

$$\lim_{t\to\infty}\psi(t)=\frac{1}{t^{\mu}} \tag{2.18}$$

with $2<\mu<3$. This waiting time distribution refers to the sojourn of the trajectories in the region at the border between the chaotic sea and the ordered islands corresponding to the accelerated modes. They find the following essential properties.

(i) The probability distribution $P(x,t)$ rescales as follows:

$$P(x,t)=\frac{1}{t^{1/(\mu-1)}}F\left[\frac{x}{t^{1/(\mu-1)}}\right] . \tag{2.19}$$

(ii) At large distances the function $F(y)$ is characterized by long tails,

$$\lim_{y\to\infty}F(y)\approx\frac{1}{y^{\mu}} . \tag{2.20}$$

(iii) The long-time limit of the correlation function $\Phi_{\xi}(t)$ is given by

$$\lim_{t\to\infty}\Phi_{\xi}(t)\approx\frac{1}{t^{\mu-2}} . \tag{2.21}$$

(iv) The long-time limit of the second moment is given by

$$\lim_{t\to\infty}\langle x^2(t)\rangle\approx t^{2H} \tag{2.22}$$

with

$$H=2-\mu/2 . \tag{2.23}$$

All these properties can be readily predicted by means of the above ME approach. The properties (i) and (ii) are immediately derived from the Lévy-like structure (2.16), the well known rescaling properties, and space asymptotic properties of the Lévy statistics [12,13].

The properties (iii) and (iv) can be easily derived by the joint use of (2.16) and the standard dynamical approach to diffusion. We note that the mere integration of (1.1) with the unique assumption that the process ξ is stationary leads [23] to (1.3). By Laplace transforming (1.3) and comparing the result for $\langle\hat{x}^2(s)\rangle$ with that derived using $\hat{P}(k;s)$ of Eqs. (2.12) and (2.13) we obtain

$$\Phi_{\xi}(t)=\frac{t^2\psi(t)}{2\langle t\rangle\langle\xi^2\rangle_{\rm eq}} , \tag{2.24}$$

which immediately accounts for (2.21). Then the property (iv) is obtained by differentiating (2.22) twice with respect to time and comparing the resulting expression to the second time derivative of (1.3). This shows clearly that the numerical results of Mori and co-workers [20] must be regarded as the first dynamical realization of a Lévy process, thereby supporting the more recent findings of Klafter, Zumofen, and Shlesinger and Zumofen and Klafter [22]. In the remaining part of this paper we shall focus on the dynamical model of Sec. III rather than on the standard map.

It must be pointed out that (2.24) provides the correct asymptotic properties of the correlation function $\Phi_{\xi}(t)$, but not an exact agreement with the results (1.3) and (1.4). Of the three models mentioned only the VM gives exact agreement with these dynamical predictions.

III. THE DYNAMICAL MODEL

The discrete time dynamical model studied herein is one of the two discussed in the recent paper by Zumofen and Klafter [15], originally introduced by Geisel, Nierwelberg, and Zacherl [6(a)]. We focus on the map they used to discuss anomalous diffusion that evolves faster than normal. Using the property of antisymmetry by reflection around $x=0$ and the invariance by translation of a unit distance, they express their map in the reduced range $0\le x\le\frac{1}{2}$, where

$$x_{n+1}=g(x_n) , \tag{3.1}$$

with

$$g(x)=(1+\lambda)x+ax^z,\quad 0\le x\le\tfrac{1}{2} . \tag{3.2}$$

They choose the constant to be $a=2^z(1-\lambda/2)$.

We define the reduced map [15]

$$\begin{aligned}&\tilde{x}_{n+1}=\tilde{g}(\tilde{x}_n),\quad 0<\tilde{x}<1 ,\\ &N_{n+1}=\hat{g}(\tilde{x}_n)+N_n .\end{aligned} \tag{3.3}$$

The coordinate x of the trajectory has been decomposed into the box number N and the position $\tilde{x}$ within a box ($x_n=N_n+\tilde{x}_n$). $\tilde{g}(\tilde{x})$ is the reduced map for the reduced

coordinate $\bar{x}$ illustrated in Fig. 1 and $\hat{g}(\bar{x})$ is used to increase or decrease the box number N by unity. We are now in a position to express the variable velocity ξ of Sec. II in terms of the mapping variable. This is given by $\xi=2\bar{x}-1$.

By adopting this procedure to make the numerical calculations we allow the velocity of the particle to also attain values distinct from 1 and -1. However, we note that the closer the particle is to the left border of the left laminar region or to the right border of the right laminar region, the larger is the time spent in the corresponding laminar region. Consequently, the resulting dynamics is slightly different from the case where the variable ξ has only the states 1 and -1, with the same inverse power-law distribution $\psi(t)$ in each of them. The unperturbed dynamics of the map is obtained by setting $\lambda=0$.

The numerical calculations are made by direct numerical implementations of the Zumofen-Klafter map [see Eqs. (3.1)–(3.3)]. The dynamics of the map is computed by means of the recursion relation given by the reduced map (Fig. 1) with the additional assumption that when the particle is found in the left laminar region the cell indicator N is decreased by one unit, and when it is found in the right laminar region the cell indicator N is augmented by one unit.

The nonstationary condition is realized as follows. The initial values of the reduced map are chosen randomly in the [0,1] interval and the iteration is repeated 10 000 times. The average is taken over 10 000 trajectories.

The stationary condition is assured by observing diffusion after ensuring that the transient process concerning the velocity ξ is over. In other words, the stationary condition is realized by choosing random initial conditions in the [0,1] interval and letting the reduced map evolve throughout the whole regime of regression of velocity to equilibrium for a transient time T_{relax} while keeping the cell indicator $N=0$, namely, preventing diffusion from taking place. After the time T_{relax} one lets the cell indicator N evolve according to Eqs. (3.1)–(3.3), the iteration is repeated 10 000 times and the average is taken over 10 000 trajectories. One determines the transient time T_{relax} by observing how long it takes for the average of the reduced map starting from a nonstationary initial condition to reach its stationary value. The transient time strongly depends on μ; for example, for $\mu=2.5$ we find that $T_{\text{relax}}=1000$ is a proper choice.

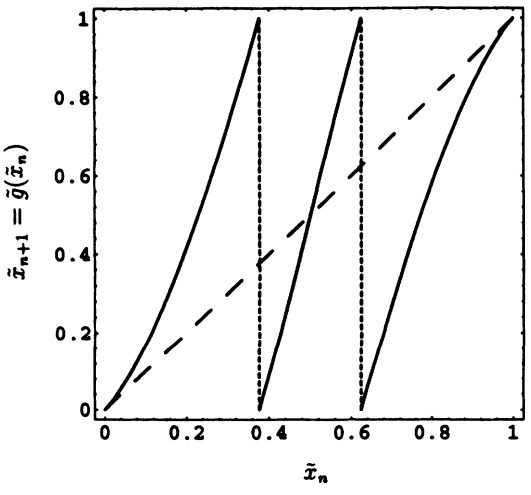

FIG. 1. Reduced map defined by (3.3) with $z=\frac{5}{3}$.

IV. THE UNPERTURBED TIME EVOLUTION OF THE SECOND MOMENT

The second moment of a process can be obtained from the second derivative of the characteristic function. This procedure is reviewed in Appendix D where we obtain the following predictions for the second moment $\langle x^2(t)\rangle$.

The ME approach results in

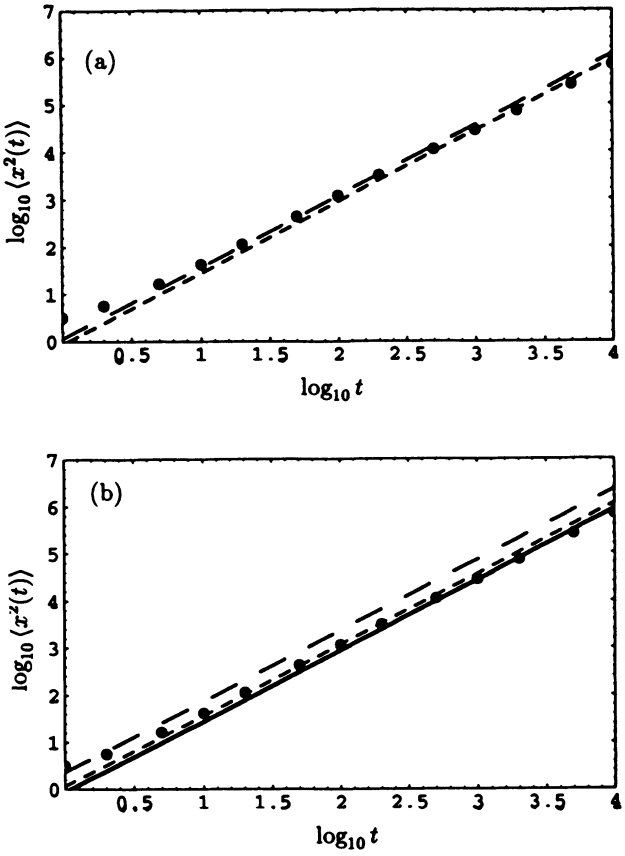

FIG. 2. Evolution of the second moment $\langle x^2(t)\rangle$ of the dynamical process (3.1)–(3.3) with $z=\frac{5}{3}$. (a) Nonstationary condition: The dots show the results of numerical calculations; the short-dashed and the long-dashed lines are the predictions of the JM approach (4.1), and of the VM approach (4.2), respectively (the numerical calculations are made according to the nonstationary prescription illustrated in Sec. III, and the VM and JM are evaluated according to the nonstationary prescription of Appendix D). (b) Stationary condition: The dots show the results of numerical calculations, the solid line shows the prediction of the ME theory, the short-dashed curve denotes the prediction of the JM approach (4.3), and the long-dash line denotes the prediction of the VM theory (4.4) (the numerical calculations are made according to the stationary prescription illustrated in Sec. III, and the VM and JM are evaluated according to the stationary prescription of Appendix D).

$$\langle x^2(t)\rangle = \frac{(\mu-1)(\mu-2)}{(4-\mu)(3-\mu)} B^{\mu-2} t^{4-\mu} . \tag{4.1}$$

As far as the JM and the VM approaches are concerned, let us consider first the nonstationary case. The JM approach results in a prediction coincident with (4.1). The VM approach results in

$$\langle x^2(t)\rangle = \frac{2(\mu-2)}{(4-\mu)(3-\mu)} B^{\mu-2} t^{4-\mu} , \tag{4.2}$$

which differs from (4.1) by a numerical factor.

Let us now consider the stationary case. The JM approach leads to

$$\langle x^2(t)\rangle = \frac{2(\mu-2)}{(4-\mu)(3-\mu)} B^{\mu-2} t^{4-\mu} \tag{4.3}$$

and the VM yields

$$\langle x^2(t)\rangle = \frac{2}{(4-\mu)(3-\mu)} B^{\mu-2} t^{4-\mu} . \tag{4.4}$$

All theories result in the same time exponent for anomalous diffusion. This is consistent with the results of numerical experiments [see Figs. 2(a) and 2(b)]. However, there are differences between the two prefactors. To check the accuracy of these predictions with the numerical "experiments" we proceed as follows. We factor out the time dependence from the second moment $\langle x^2(t)\rangle$ and define the coefficient function

$$g(\mu) \equiv \frac{\langle x^2(t)\rangle}{t^{4-\mu}} . \tag{4.5}$$

Thus, from the numerical evaluation of the second moment we define the function $g(\mu)$, which is then compared to the predictions stemming from (4.1)–(4.4) with B assigned by (2.5). From Fig. 3(a) we see that in the nonstationary case the prediction of the JM approach is slightly closer to the results of the numerical experiment than the prediction of the VM approach. In the stationary case, we see from Fig. 3(b) that the ME is the theory whose predictions are closest to the numerical results.

It is remarkable that all three theories result in a divergence at $\mu=3$, which is not consistent with the results of the numerical experiment. Notice that the direct integration of (1.3), supplemented by (1.4), leads to the same result as the VM theory, (4.4). This is a remarkable aspect of the VM, but it also casts doubt on the accuracy of (1.4), since this theory shares with the VM, and with all the other theories, the divergence at $\mu=3$. This would suggest that none of the three theories, nor (1.4), is entirely correct for all values of the parameter μ.

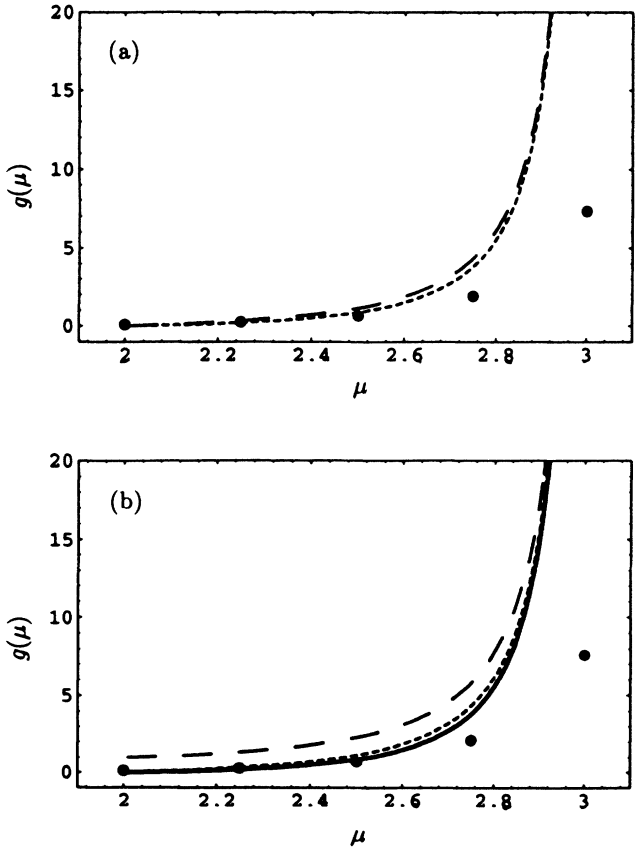

FIG. 3. $g(\mu)$ coefficient function defined by (4.5) in both the nonstationary (a) and stationary (b) cases. The dots show the results of numerical calculations in the corresponding conditions. The long-dashed lines and the short-dashed lines denote the prediction of the VM and the JM theories, in the corresponding conditions. The solid line of (b) denotes the prediction of the ME approach.

V. RESPONSE TO PERTURBATION

We study here the problem of the response of the map to two different kinds of perturbation, geometrical and dynamical. We focus our attention on the first moment of the x distribution, which in the absence of perturbations would vanish. We consider two different ways of observing the response to these perturbations, nonstationary and stationary. The former refers to an initial condition for the dynamical system of Sec. III, with the velocity ξ uniformly distributed in the interval $[-1,1]$. We could assess that the response in this case is essentially equivalent to adopting an initial condition with the velocity in the equilibrium distribution in the absence of perturbation. Thus, from a physical point of view this choice corresponds to a case where the perturbation is abruptly applied to a sample of diffusing particles in a stationary state. The second choice refers to the case where the variable velocity is given an initial distribution at equilibrium with respect to the map in the presence of the perturbation.

In Appendix E we provide the details of the calculations leading to the analytical expressions for the first moment of the response here reported. The calculations are made using two different methods.

(i) The first method consists of making the strength of the perturbation tend to zero, expanding the Laplace transform of $\langle x(t)\rangle$ with respect to this perturbation strength, and keeping only the lowest-order contribution. Then as time tends to infinity, namely, s tends to zero, the lowest-order contribution with respect to s is considered. This approach can be applied to all the models in both the nonstationary and stationary conditions but the VM

in the stationary state.

(ii) The second method consists of applying the procedure (i) in the reversed order, making s tend to zero first, and then making the perturbation strength tend to zero.

In the case of the geometrical perturbation the results turned out to be independent of the method adopted. In the case of the dynamical perturbation, on the contrary, the first method results in a response which coincides with that expected on the basis of the Green-Kubo argument (1.17), and the second method leads to a prediction which fits the expectation of the stationary treatment.

A. Geometric bias

The first perturbation of the map consists in changing the size of its left laminar region (see Fig. 1) by the quantity p. This has the effect of changing the parameter B in the left laminar region by the quantity η, which is determined using simple geometrical arguments (see Appendix F). Thus the perturbed waiting time distribution reads as follows:

$$\psi(x,t)=\tfrac{1}{2}\delta(x-t)\psi(t)+\tfrac{1}{2}\delta(x+t)\psi_\eta(t)\ , \tag{5.1}$$

where $\psi(t)$ is the unperturbed waiting time distribution and $\psi_\eta(t)$ is the perturbed one, defined by

$$\psi_\eta(t)=\frac{A_\eta}{(B-\eta+t)^\mu}\ , \tag{5.2}$$

where (see Appendix F)

$$\eta=(\mu-1)\left[1+\frac{2\mu}{\mu-1}\right]p\ . \tag{5.3}$$

Notice that both $\psi(t)$ and $\psi_\eta(t)$ are normalized, namely,

$$A_\eta=(\mu-1)(B-\eta)^{\mu-1}\ . \tag{5.4}$$

This guarantees the global normalization

$$\int_{-\infty}^{\infty}dx\int_0^\infty dt\ \psi(x,t)=1\ . \tag{5.5}$$

The calculations outlined in Appendix E lead to the following conclusion. The response to the perturbed waiting time distribution is the same for the three theories, in both the stationary and nonstationary conditions, and is expressed by

$$\langle x(t)\rangle=\frac{\eta}{2B}t\ . \tag{5.6}$$

Figure 4 compares this theoretical prediction to the result of the numerical experiment in the case $\mu=2.5$. Both theory and numerical experiment result in a linear dependence of the response on time. On this issue, the agreement between theory and numerical experiment is remarkable. However the slope of the numerical experiment is about twice that of the theoretical prediction. To assess the μ dependence of this disagreement we again define a coefficient function

$$f(\mu)\equiv\frac{\langle x(t)\rangle B}{\eta t}\ , \tag{5.7}$$

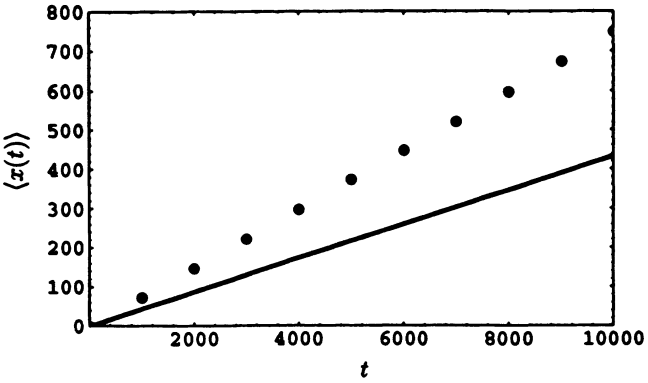

FIG. 4. First moment of x as a function of time. This is the response of map (3.1)–(3.3) with $z=\frac{5}{3}$ to the perturbation with geometric bias. The average is taken over 10 000 trajectories whose initial conditions are randomly chosen in the interval [0,1]. The dots show the results of numerical calculations and the solid line is the prediction of the ME approach. Note that the ME prediction coincides with those of the JM and VM approaches.

which, according to (5.6), should be independent of μ and yield

$$f(\mu)=\tfrac{1}{2}\ . \tag{5.8}$$

This prediction is compared to the numerical results in Fig. 5, and for both theory and numerical "experiment" results in horizontal straight lines. We see that there is a good qualitative agreement between the ME, JM, and VM predictions and the numerical experiment, while the quantitative agreement is not satisfactory.

B. Dynamical bias

A dynamical bias is obtained by driving the left laminar region with the perturbed map (3.2) with a nonvanishing value of λ. Using Eq. (67) of Ref. [15], we obtain the following perturbed expression for the waiting time distribution:

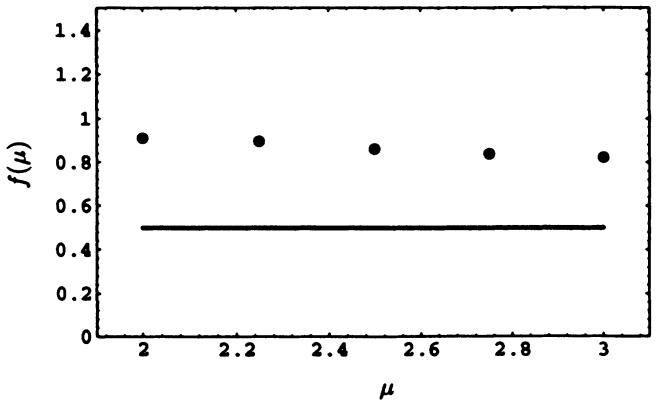

FIG. 5. $f(\mu)$ coefficient function defined by (5.7). The dots show the results of numerical calculations and the solid line is the prediction of the theory.

$$\psi(t)=\frac{2\exp[\lambda t/(\mu-1)]}{(1+(2/\lambda)\{\exp[\lambda t/(\mu-1)]-1\})^{\mu}} . \quad (5.9)$$

At $\lambda=0$, we recover the form (2.3) with (2.4) and (2.5). By expanding (5.9) up to the first order in λ, we obtain

$$\psi(t)\cong\frac{A}{(B+t)^{\mu}}\left[1+\frac{\lambda t}{\mu-1}\left[1-\frac{\mu}{2}\frac{t}{(B+t)}\right]\right] . \quad (5.10)$$

In the limiting case of extremely weak λ's the response to this kind of perturbation turns out to be independent of whether the perturbed waiting time distribution has the form (5.9) or the form

$$\psi_{\varepsilon}(t)=\frac{A_{\varepsilon}}{(B+t)^{\mu}}\exp(-\varepsilon t) , \quad (5.11)$$

provided that the damping ε is related to λ by

$$\varepsilon=\lambda\frac{(\mu-2)}{2(\mu-1)} . \quad (5.12)$$

The expression for the perturbed waiting time distribution (5.11) is related to (5.9) through (5.12).

Applying the method (i) we obtain the following results. For the ME, and for the JM approach in the nonstationary case, we obtain for the average displacement

$$\langle x(t)\rangle=\frac{\varepsilon}{2}\frac{(\mu-1)(\mu-2)}{(4-\mu)(3-\mu)}B^{\mu-2}t^{4-\mu} . \quad (5.13)$$

The stationary expression for the JM is given by

$$\langle x(t)\rangle=\frac{\varepsilon}{2}\frac{(\mu-1)}{(4-\mu)(3-\mu)}B^{\mu-2}t^{4-\mu} . \quad (5.14)$$

The VM approach in the nonstationary case leads to

$$\langle x(t)\rangle=\frac{\varepsilon}{2}\frac{(\mu-1)}{(4-\mu)(3-\mu)}B^{\mu-2}t^{4-\mu} . \quad (5.15)$$

Method (i) cannot be applied to the VM in the stationary case. By applying method (ii) we obtain

$$\langle x(t)\rangle=\varepsilon^{\mu-2}\frac{(\mu-1)\Gamma(3-\mu)}{2}B^{\mu-2}t . \quad (5.16)$$

Surprisingly, the application of method (ii) to all the other cases leads to the same result, (5.16); namely, to a conductivity constant in time.

Comparing (5.13) and (5.15) to the corresponding expressions for the unperturbed second moments, (4.1) and (4.2), we can rewrite these results as follows.

$$\langle x(t)\rangle_{\text{bias}}=\frac{\varepsilon}{2}\langle x^2(t)\rangle_0 \quad (5.17)$$

for the JM approach in the nonstationary case. The nonstationary expression for the VM implies for this model

$$\langle x(t)\rangle_{\text{bias}}=\frac{\varepsilon}{2}\frac{(\mu-1)}{2(\mu-2)}\langle x^2(t)\rangle_0 . \quad (5.18)$$

Here, to make the result more apparent, we have used the subscript "bias" to denote the first moment of the response and the subscript "0" to denote the unperturbed dynamics of the second moment.

As noted in Sec. I, the mere integration of (1.1) leads to (1.3) [23]. By replacing the expression (1.3) in (5.17) and (5.18) and by differentiating the resulting expression with respect to time, we derive a final expression with the form of the generalized Green-Kubo expression (1.17). Usually the Green-Kubo theory is applied to processes where the correlation function of the velocity is integrable, thereby resulting in transport quantities obtained by replacing the upper limit of time integration, t, with infinity. It is remarkable that the theory developed herein leads to the conclusion that the case of anomalous diffusion in the nonstationary regime can be studied with a formalism compatible with the Green-Kubo method, with the only caveat being that of relaxing the assumption that in the long-time regime the conductivity reaches a time-independent value. We see indeed that our theoretical derivation leads to a conductivity which is a steadily increasing function of time.

This is confirmed by Fig. 6, showing the dependence of

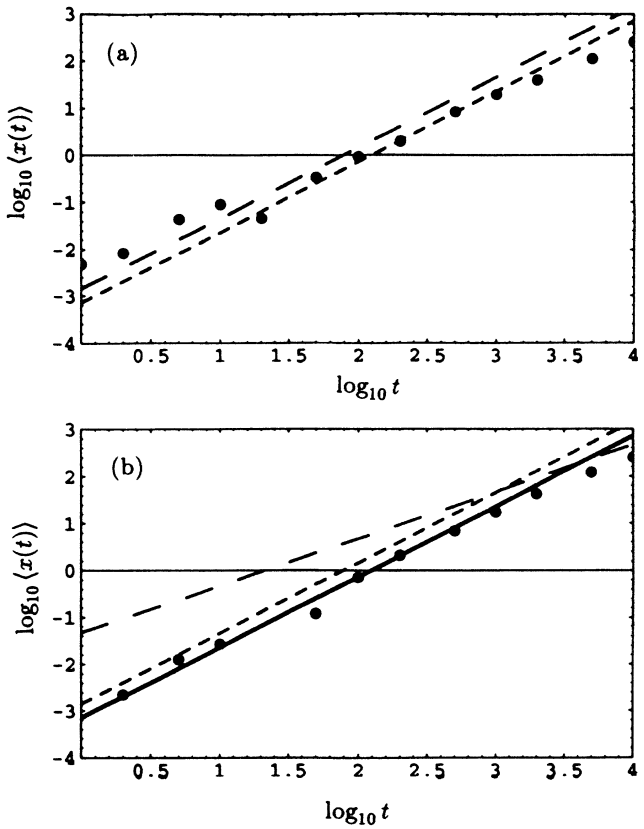

FIG. 6. Response of map (3.1)–(3.3) to the dynamical perturbation with $z=\frac{5}{3}$. (a) Nonstationary condition. The dots denote the results of the computer calculations corresponding to a flat initial distribution for ξ. The short-dashed line denotes the prediction of the nonstationary JM approach. The long-dashed line is the prediction of the VM theory in the nonstationary case. (b) Stationary case. The dots correspond to the computational results obtained adopting the stationary prescription illustrated in Sec. III. The long-dashed line shows the prediction of the VM theory in the stationary case [coinciding with that of all the theories resting on the application of method (ii)]. The short-dashed line denotes the prediction of the JM theory in the stationary case, (5.14). The solid line corresponds to the prediction of the ME theory by means of method (i).

the first moment of the response on $t^{4-\mu}$ in the early part of the nonstationary process (a), and the linear dependence on time in the stationary state in the presence of perturbation (b). Figure 6 refers to the case with $\mu=2.5$ and $\lambda=0.01$.

We devote special attention to the nonstationary case, resulting in the nonlinear dependence of the first moment on time. After assessing with Fig. 6(a) that the power of the response is that predicted by the theory in the corresponding nonstationary condition, we make the following more refined comparison. We numerically evaluate $\langle x(t)\rangle_{\text{bias}}$ and $\langle x^2(t)\rangle_0$. Then we determine their ratio

$$h(\mu)\equiv\frac{\langle x(t)\rangle_{\text{bias}}}{\lambda\langle x^2(t)\rangle_0} \tag{5.19}$$

and compare the numerical result to the theoretical predictions

$$h(\mu)=\frac{1}{4}\frac{(\mu-2)}{(\mu-1)} \tag{5.20}$$

of the JM approach and

$$h(\mu)=\tfrac{1}{8} \tag{5.21}$$

of the VM approach. The result of this comparison is shown in Fig. 7. The JM result is in quantitative and qualitative agreement with the results of numerical calculations which is significantly closer to the numerical result than that of the VM approach.

C. Comments on the response of anomalous diffusion to perturbation

The long-time drift U produced by the perturbation can be evaluated with straightforward arguments. Let us consider the geometric perturbation first. The statistical weight of the perturbed and unperturbed states of the velocity, namely, those concerning the perturbed and the unperturbed laminar regions, respectively, are given by

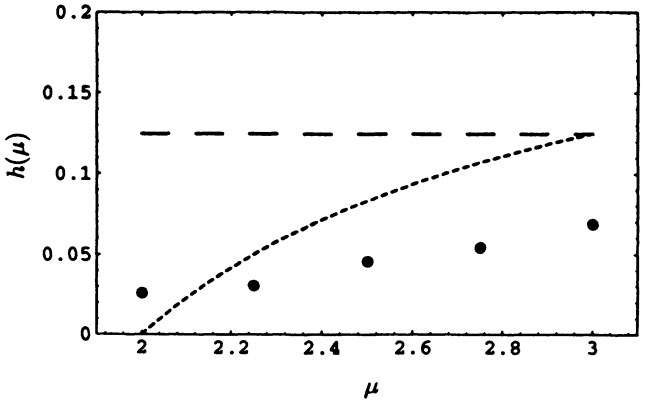

FIG. 7. $h(\mu)$ coefficient function defined by (5.19). The dots show the results of numerical calculations, the short-dashed line is the prediction of the JM theory, and the long-dashed line denotes that of the VM approach. The JM and the VM approaches refer to the nonstationary case. The "stationary" ME theory, with method (i), would coincide with the short-dashed line.

$$P_\eta=\frac{\langle t_\eta\rangle}{\langle t_\eta\rangle+\langle t\rangle} \tag{5.22}$$

and

$$P_0=\frac{\langle t\rangle}{\langle t_\eta\rangle+\langle t\rangle}\ , \tag{5.23}$$

where

$$\langle t_\eta\rangle=\int_0^\infty dt\, t\psi_\eta(t) \tag{5.24}$$

and $\langle t\rangle$ is the usual mean time of the unperturbed laminar region. We thus obtain

$$U=\frac{\langle t\rangle-\langle t_\eta\rangle}{\langle t\rangle+\langle t_\eta\rangle}\ . \tag{5.25}$$

The long-time drift in the dynamical case is obtained from (5.25) by replacing $\langle t_\eta\rangle$ with $\langle t_\varepsilon\rangle$, the mean waiting time within the laminar region under the action of the dynamical perturbation.

For the geometric bias we have

$$\langle t_\eta\rangle=\frac{B-\eta}{\mu-2}\ . \tag{5.26}$$

In the case of the dynamical bias, at the lowest order in ε we have

$$\langle t_\varepsilon\rangle\cong\langle t\rangle-\frac{\mu-1}{\mu-2}\Gamma(3-\mu)B^{\mu-1}\varepsilon^{\mu-2}\ . \tag{5.27}$$

Consequently, in the case of the geometric bias we obtain

$$U=\frac{\eta}{2B} \tag{5.28}$$

and in the case of the dynamical bias, still at the lowest order in ε,

$$U=\varepsilon^{\mu-2}\frac{(\mu-1)\Gamma(3-\mu)B^{\mu-2}}{2}\ . \tag{5.29}$$

It is remarkable that (5.28) corresponds to the predictions of all three theories, in both the stationary and the nonstationary regimes, and that (5.29) is the drift predicted by all the theories if method (ii) is applied; see (5.16).

We are thus led to the following, very simple interpretation of the process of the response to perturbations. The nonstationary prediction corresponds to an abrupt application of the perturbation to the system undergoing a stationary unperturbed diffusion. This would imply an initial condition with the velocity at equilibrium under the action of no bias. However, the power of the time dependence of the nonstationary process is essentially independent of whether we use as the initial condition the unperturbed equilibrium distribution of the velocity or a merely flat distribution. Thus we can apply to this latter condition the same arguments as those we would apply to a real experimental perturbation resting on the abrupt application of the perturbation to a sample of particles in a state of free diffusion.

Due to the fact that the regression of velocity to equilibrium is expected to be as slow as its equilibrium correlation function, the whole process of diffusion takes place

in a nonequilibrium configuration. All the nonstationary theories refer to this kind of diffusion process. As slow as it is, this kind of diffusion process does not last forever. In the region of extremely large times, when the variable velocity becomes close to the final equilibrium condition, the diffusion process becomes stationary and the first moment $\langle x(t) \rangle$ increases linearly in time with a rate given by the time-independent drift U.

The first part of the response process can be described by a Green-Kubo formula. However, since the correlation function of the velocity is not integrable between zero and infinity, the resulting conductivity turns out to increase as a function of time.

The system slowly moves from this slow but transient condition into the stationary regime, which is then described by a time-independent conductivity. In spite of the fact that in the long-time regime a time-independent conductivity is recovered, this cannot fit the prescriptions of the Green-Kubo approach. In this long-time regime the Green-Kubo approach would lead to an infinite conductivity, and the finite values for the conductivities (5.28) and (5.29) cannot be derived from the Green-Kubo relation involving the equilibrium autocorrelation function of the velocity ξ.

It must be remarked that not all the possible kinds of perturbations can trigger the anomalous Green-Kubo response process of (1.17). For this to take place it is necessary to perturb the velocity distribution in the region where the regression to equilibrium is extremely slow. The geometrical perturbation, on the contrary, perturbs the velocity distribution in the regions close to the internal border of the laminar region, where the regression to equilibrium is very fast. This is the reason why all the theories, in both the stationary and nonstationary regimes, result in the same prediction. The process of regression to equilibrium is so fast as to make the diffusion process stationary over all the time region explored. The rapidity of the regression to equilibrium is also the reason why the diffusion process turns out to be scarcely dependent on the details of the microscopic process. The different theories imply different "microscopic" processes, but, due to the fact that the "macroscopic" process is insensitive to the microscopic details, they result in the same long-time prediction.

VI. CONCLUDING REMARKS

A derivation of the Lévy distribution has been presented based on the ME. Although this approach is not yet a rigorous derivation of the Lévy processes from dynamics, it provides all the correct asymptotic properties for the velocity correlation function, and for the second moment and tails of the probability distribution of x in terms of the waiting time distribution $\psi(t)$.

The ME method is not yet as good as the VM approach, which leads to exact agreement with the dynamical prediction (1.3) supplemented by the expression for the correlation function of the velocity (1.4). The purpose of future investigations should be that of deriving the ME directly from the Liouvillian picture [5] or, in the case of mappings, from the Perron-Frobenius equation [30].

We have focused our attention on the parameter region $2 < \mu < 3$, because the ME is tailored for this region. It is straightforward to assess that all three theories, in both the stationary and nonstationary regimes, result in the same reasonable predictions for $\mu > 3$. This can be traced back to the fact that for $\mu > 3$ there exists a finite second moment of $\psi(t)$. However, all three theories result in a divergence for $\mu \to 3$ from the region $2 < \mu < 3$, which is not consistent with the numerical results. Numerical experiment shows these divergences to be unphysical, and the problem of how to suppress them will be the subject of a future publication.

The treatment of the response to perturbations presented here will hopefully lead to new theoretical insights into the evolution of dynamical systems. The problem of the linear response of maps has already been the subject of investigation by several authors (see, for instance, [31] and [32]). However, the preceding researchers were essentially focused on the response of a map variable, such as the velocity ξ, which is constrained to move in a bounded interval, rather than on the diffusing variable x associated with the velocity ξ. Another difference is the fact that the perturbation is applied to a variable ξ which is here a source of anomalous rather than normal diffusion.

We have seen that a linear response treatment in this anomalous condition is still possible. However, this conflicts with the Kubo perturbation treatment. In the early part of the process the conductivity turns out to be an increasing function of time, thereby driving the system towards physical conditions more and more incompatible with the Kubo [33,28] perturbation treatment, which aims at expressing the response in terms of the unperturbed correlation function of the velocity. We have seen that in the stationary long-time limit the response is controlled by a transport parameter which does not have anything to do with the velocity correlation function, as in the conventional Kubo [33,28] treatment. As a final comment, we would like to stress that the VM theory conflicts with the application of method (i) and, thus, with the possibility of recovering a Green-Kubo structure. This might be a sign of the strength rather than the weakness of this theory, which is proved to fit the dynamical constraints (1.3) and (1.4) and is thus expected to reproduce rigorously the stationary dynamical condition even in the presence of perturbation.

ACKNOWLEDGMENT

One of us (B.J.W.) would like to thank the Office of Naval Research for partial support of this work.

APPENDIX A

The choice of T as the first moment of the waiting time distribution (2.11) is dictated by the fact that this is the only characteristic time scale available in the region $2 < \mu < 3$, compatible with the existence of Lévy processes. Note that the first moment of the distribution is the only finite one of integer value.

In addition to this intuitive argument, we can also

adopt random walk arguments. As we have mentioned in the Introduction, we derived the Lévy distribution from a ME approach without recourse to random walks. Therefore the remarks of this Appendix may be regarded as a check of this choice of T, rather than being the only plausible justification for (2.11).

The theoretical developments carried out here are similar to those used by Wang [29] but they are adapted to our specific need of determining accurate numerical factors. Let us denote by $p(t)$ the probability that a jump from one site to another occurs (if we use the JM) or the probability that the particle stops and starts moving in a randomly chosen new direction (if we use the VM). The mean value of jumps occurring in the time interval ranging from 0 to t, denoted by $N(t)$, is given by

$$N(t)=\int_0^t p(t')dt' \ . \tag{A1}$$

Therefore the rate we wish to determine is

$$\frac{1}{T}=\lim_{t\to\infty}\frac{N(t)}{t} \ . \tag{A2}$$

Note that $p(t)$ is derived from random walk arguments as follows. We write

$$p(t)=\int_{-\infty}^{\infty} Q(x,t)dx \ , \tag{A3}$$

where $Q(x,t)$ is the probability for the particle to arrive at the site x at time t, and to stop before changing direction. Using Eq. (7) of Ref. [15] we see that $\hat{Q}(k,s)$ can be expressed in the following form:

$$\hat{Q}(k,s)=\frac{1}{1-\hat{\psi}(k,s)} \ . \tag{A4}$$

Thus using (A3) we obtain

$$\hat{p}(s)=\hat{Q}(0,s)=\frac{1}{1-\hat{\psi}(s)} \ , \tag{A5}$$

so that in the asymptotic regime

$$p(t)=\frac{1}{\langle t\rangle} \ , \tag{A6}$$

where $\langle t\rangle$ is the first moment of the waiting time distribution $\psi(t)$. In conclusion we derive

$$T=\langle t\rangle \tag{A7}$$

supporting our choice in (2.11).

APPENDIX B

This Appendix is devoted to adapting the probability distribution of the JM to the stationary condition. Following Haus and Kehr [18], we express the probability distribution of the JM as

$$\hat{P}(k,s)=\frac{\hat{h}(k,s)\hat{\Psi}(s)}{1-\hat{\psi}(k,s)}+\hat{H}(s) \ , \tag{B1}$$

where

$$\hat{\Psi}(s)=\frac{1-\hat{\psi}(0,s)}{s} \ , \tag{B2}$$

$$\hat{H}(s)=\frac{1-\hat{h}(0,s)}{s} \ , \tag{B3}$$

and $h(x,t)$ denotes the probability for moving a distance x in time t in the first motion event. To proceed, we have to make a proper choice for $h(x,t)$, corresponding to stationary initial conditions.

To make this choice, we note that Eq. (3.3) of Ref. [18] gives the distribution $h(t)$ corresponding to stationary conditions for the case of a decoupled $\psi(x,t)$. It reads

$$h(t)=\frac{\Psi(t)}{\langle t\rangle} \ , \tag{B4}$$

where

$$\Psi(t)=\int_t^{\infty} dt'\psi(t') \ . \tag{B5}$$

We generalize (B4) to the case of our space-time coupled $\psi(x,t)$ in the following way:

$$h(x,t)=\frac{\Psi(x,t)}{\langle t\rangle} \ , \tag{B6}$$

where

$$\Psi(x,t)=\tfrac{1}{2}\delta(|x|-t)\Psi(t) \ . \tag{B7}$$

This is the same choice as that adopted in Refs. [16] and [17] for the VM to define $h(x,t)$. Notice that Haus and Kehr choose another generalization of (B4); see Eq. (3.16) of Ref. [18]. That choice is not appropriate here, because the waiting time distributions $\psi(t)$ considered in this paper do not have a finite second moment, and with the choice of Haus and Kehr this would lead to a diverging second moment $\langle x^2(t)\rangle$.

APPENDIX C

The purpose of this Appendix is to provide details on the calculations leading to the asymptotic expression for the probability distribution, and the value (2.17) for the parameter b. We have seen in Sec. II that the ME approach leads to the following expression for the Fourier-Laplace transform of the probability distribution $P(x,t)$:

$$\hat{P}(k,s)=\frac{1}{s-\hat{K}(k,s)} \ . \tag{C1}$$

It is interesting to remark that this structure, and the important detailed balance condition

$$\hat{K}(0,s)=0 \ , \tag{C2}$$

are shared by the three theories.

As far as the ME approach is concerned, from Sec. II we derive

$$\hat{K}(k,s)=\frac{\hat{\psi}(k,s)-\hat{\psi}(s)}{T} \ . \tag{C3}$$

Equations (10) and (11) of Ref. [15] give for the nonstationary JM

$$\hat{K}(k,s)=\frac{\hat{\psi}(k,s)-\hat{\psi}(s)}{\hat{\Psi}(s)} \ ; \tag{C4}$$

and for the nonstationary VM

$$\hat{K}(k,s)=s+\frac{\hat{\psi}(k,s)-1}{\hat{\Psi}(k,s)} . \tag{C5}$$

$\hat{\psi}(k,s)$, $\hat{\Psi}(s)$, and $\hat{\Psi}(k,s)$ are given by [15]

$$\hat{\psi}(k,s)=\int_0^\infty dt\,\exp(-st)\cos(kt)\psi(t) , \tag{C6}$$

$$\hat{\Psi}(s)=\int_0^\infty dt\,\exp(-st)\int_t^\infty dt'\psi(t')=\frac{1-\hat{\psi}(s)}{s} , \tag{C7}$$

$$\hat{\Psi}(k,s)=\int_0^\infty dt\,\exp(-st)\cos(kt)\int_t^\infty dt'\psi(t') . \tag{C8}$$

From Eq. (20) of Ref. [17] we get for the stationary VM

$$\hat{K}(k,s)=s-\frac{\langle t\rangle[1-\hat{\psi}(k,s)]}{[\hat{\Psi}(k,s)]^2+\langle t\rangle[1-\hat{\psi}(k,s)]\hat{H}(k,s)} , \tag{C9}$$

where $\hat{H}(k,s)$ is given by [16]:

$$\hat{H}(k,s)=\frac{1}{\langle t\rangle}\int_0^\infty dt\,\exp(-st)\cos(kt) \times\int_t^\infty dt'(t'-t)\psi(t') . \tag{C10}$$

Using Eqs. (B1) and (B6) we get

$$\hat{K}(k,s)=s-\frac{\langle t\rangle[1-\hat{\psi}(k,s)]}{\hat{\Psi}(k,s)\hat{\Psi}(s)+\langle t\rangle[1-\hat{\psi}(k,s)]\hat{H}(s)} , \tag{C11}$$

where

$$\hat{H}(s)=\frac{1}{s}\left[1-\frac{\hat{\Psi}(s)}{\langle t\rangle}\right] . \tag{C12}$$

We are thus in a position to prove the detailed balance condition (C2) also for (C4), (C5), (C9), and (C11) using the properties [15] $\hat{\psi}(0,s)=\hat{\psi}(s)$, $\hat{\Psi}(0,s)=\hat{\Psi}(s)=[1-\hat{\psi}(s)]/s$, and $\hat{H}(0,s)=\hat{H}(s)$.

Now, we make s and k tend to zero subject to the constraint $s\sim k^\alpha$ and $\alpha>1$, so that s tends to zero more quickly than does k. As pointed out in Sec. II, in the region $2<\mu<3$ this condition is necessary to establish a connection with the Lévy processes.

We also use the asymptotic expansion

$$\hat{\psi}(s)\cong 1-\langle t\rangle s-cs^{\mu-1} , \tag{C13}$$

with

$$\langle t\rangle=\frac{B}{\mu-2} \tag{C14}$$

and

$$c=\Gamma(2-\mu)B^{\mu-1} . \tag{C15}$$

Taking the limit of vanishing s and k in Eqs. (C3)–(C12) we then obtain for $\hat{K}(k,s)$, at leading order in k,

$$\hat{K}(k,s)\cong-\frac{c}{\langle t\rangle}\cos\left[\frac{\pi}{2}(\mu-1)\right]k^{\mu-1} \tag{C16}$$

for the JM and the VM approaches, both in the stationary and nonstationary regimes, whereas the ME approach leads to

$$\hat{K}(k,s)\cong-\frac{c}{T}\cos\left[\frac{\pi}{2}(\mu-1)\right]k^{\mu-1} . \tag{C17}$$

Notice that the choice we made for T with (2.11), $T=\langle t\rangle$, leads to the same value b for all three theories,

$$b=\frac{c}{\langle t\rangle}\cos\left[\frac{\pi}{2}(\mu-1)\right] , \tag{C18}$$

which coincides with the value for b given by (2.17). Equation (C18) can be rewritten using (C14) and (C15) as

$$b=-B^{\mu-2}\Gamma(3-\mu)\cos\left[\frac{\pi}{2}(\mu-1)\right] , \tag{C19}$$

from which it is easy to see that, for $2<\mu<3$, b is indeed a positive quantity.

Notice that the calculations leading to (C18), and consequently to (2.17), would also be valid in the region $1<\mu<2$ if $\alpha>1$. If α is identified with $\mu-1$, on the contrary, the approximations on which our calculation rests are invalidated, and b turns out to vanish.

APPENDIX D

Here we provide details of the calculations necessary to derive the explicit expressions for the moments, (4.1)–(4.4). The Fourier-Laplace transform of the second moment is derived from that of the probability distribution by using

$$\langle\hat{x}^2(s)\rangle=-\left[\frac{\partial^2\hat{P}(k,s)}{\partial^2 k}\right]_{k=0}=-\frac{1}{s^2}\left[\frac{\partial^2\hat{K}(k,s)}{\partial^2 k}\right]_{k=0} , \tag{D1}$$

which stems from

$$\hat{P}(k,s)=\frac{1}{s-\hat{K}(k,s)} \tag{D2}$$

under the assumption

$$\left[\frac{\partial\hat{K}(k,s)}{\partial k}\right]_{k=0}=0 , \tag{D3}$$

which is fulfilled by all theories considered here.

Supplementing (D1) with (C3), (C4), (C5), (C9), and (C11) we get

$$\langle\hat{x}^2(s)\rangle=\frac{1}{s^2}\frac{1}{\langle t\rangle}\frac{d^2\hat{\psi}(s)}{ds^2} \tag{D4}$$

for the ME;

$$\langle\hat{x}^2(s)\rangle=\frac{1}{s^2}\frac{1}{\hat{\Psi}(s)}\frac{d^2\hat{\psi}(s)}{ds^2} \tag{D5}$$

for the nonstationary JM;

$$\langle\hat{x}^2(s)\rangle=\frac{2}{\langle t\rangle s^3}\left[\hat{\Psi}(s)+\frac{d\hat{\psi}(s)}{ds}\right] \tag{D6}$$

for the stationary JM;

$$\langle\hat{x}^2(s)\rangle=\frac{2}{s^3}\frac{1}{\hat{\Psi}(s)}\left[\hat{\Psi}(s)+\frac{d\hat{\psi}(s)}{ds}\right] \tag{D7}$$

for the nonstationary VM; and

$$\langle \hat{x}^2(s) \rangle = \frac{2}{s^3} \left[1 - \frac{\hat{\Psi}(s)}{\langle t \rangle} \right] \tag{D8}$$

for the stationary VM.

Equations (4.1)–(4.4) are derived from (D4)–(D8) by using the asymptotic expansion (C13), relation (C7), and the inverse Laplace transform

$$L^{-1}(s^{\mu-5}) = \frac{t^{4-\mu}}{\Gamma(4-\mu)} = \frac{t^{4-\mu}}{(4-\mu)(3-\mu)(2-\mu)\Gamma(2-\mu)} . \tag{D9}$$

APPENDIX E

This Appendix is devoted to illustrating the calculations leading to the predictions on the response to the two different types of perturbations discussed in Sec. V. For both types of perturbations, both affecting the left laminar region, we use the following waiting time distribution:

$$\psi(x,t) = \tfrac{1}{2}\delta(x-t)\psi(t) + \tfrac{1}{2}\delta(x+t)\psi_\eta(t) , \tag{E1}$$

where $\psi_\eta(t)$ is a given perturbed distribution depending on a perturbation strength η. Throughout our calculations we use the following definition:

$$\Delta\psi(t) = \psi_\eta(t) - \psi(t) . \tag{E2}$$

We evaluate the response looking at the first moment, which vanishes in the unperturbed case. In the presence of the perturbation the first moment does not vanish, and is derived from the formula

$$\langle \hat{x}(s) \rangle = -i \left[\frac{\partial \hat{P}(k,s)}{\partial k} \right]_{k=0} = -\frac{i}{s^2} \left[\frac{\partial \hat{K}(k,s)}{\partial k} \right]_{k=0} . \tag{E3}$$

The functions $\Psi(t)$, $\Psi(x,t)$, $h(x,t)$, $H(t)$, and $H(x,t)$ which appear in the probability distributions $P(x,t)$ of the various theories are now defined by

$$\Psi(t) = \frac{1}{2}\int_t^\infty dt'\psi(t') + \frac{1}{2}\int_t^\infty dt'\psi_\eta(t') , \tag{E4}$$

$$\Psi(x,t) = \frac{1}{2}\delta(x-t)\int_t^\infty dt'\psi(t') + \frac{1}{2}\delta(x+t)\int_t^\infty dt'\psi_\eta(t') , \tag{E5}$$

$$h(x,t) = \frac{\Psi(x,t)}{\langle t \rangle} , \tag{E6}$$

$$H(t) = \frac{1}{\langle t \rangle}\left[\frac{1}{2}\int_t^\infty dt'(t'-t)\psi(t') + \frac{1}{2}\int_t^\infty dt'(t'-t)\psi_\eta(t') \right] , \tag{E7}$$

$$H(x,t) = \frac{1}{\langle t \rangle}\left[\frac{1}{2}\delta(x-t)\int_t^\infty dt'(t'-t)\psi(t') + \frac{1}{2}\delta(x+t)\int_t^\infty dt'(t'-t)\psi_\eta(t') \right] . \tag{E8}$$

Thus we can express (E3) in terms of $\Delta\psi$ at the lowest order in η as follows:

$$\langle \hat{x}(s) \rangle = \frac{1}{2s^2}\frac{1}{\langle t \rangle}\frac{d}{ds}\Delta\hat{\psi}(s) \tag{E9}$$

for the ME;

$$\langle \hat{x}(s) \rangle = \frac{1}{2s^2}\frac{1}{\hat{\Psi}_0(s)}\frac{d}{ds}\Delta\hat{\psi}(s) \tag{E10}$$

for the nonstationary JM;

$$\langle \hat{x}(s) \rangle = \frac{1}{2\langle t \rangle}\frac{\Delta\hat{\psi}(s)}{s^3} \tag{E11}$$

for the stationary JM;

$$\langle \hat{x}(s) \rangle = \frac{1}{2s^2}\frac{1}{\hat{\Psi}_0(s)}\frac{\Delta\hat{\psi}(s)}{s} \tag{E12}$$

for the nonstationary VM; and

$$\langle \hat{x}(s) \rangle = \frac{1}{2\langle t \rangle s^2}\frac{d}{ds}\Delta\hat{\psi}(s=0) \tag{E13}$$

for the stationary VM.

Note that with $\hat{\Psi}_0(s)$ we denote $\hat{\Psi}(s)$ in the unperturbed case, namely,

$$\hat{\Psi}_0(s) = \frac{1-\hat{\psi}(s)}{s} . \tag{E14}$$

To proceed further we must consider the specific kind of perturbation under study.

1. Geometric bias

In this case we have

$$\psi_\eta(t) = \frac{A_\eta}{(B-\eta+t)^\mu} . \tag{E15}$$

In this case, at the lowest order in η and in the limit of very small s, we obtain

$$\Delta\hat{\psi}(s) \cong \eta\left[\frac{s}{\mu-2} + \frac{(\mu-1)c}{B}s^{\mu-1} \right] \tag{E16}$$

and

$$\hat{\Psi}_0(s) \cong \langle t \rangle . \tag{E17}$$

By replacing (E16) and (E17) into (E9)–(E13) we obtain for all theories

$$\langle x(t) \rangle = \frac{\eta}{2B}t . \tag{E18}$$

2. Dynamical bias

Let us consider the perturbed waiting time distribution

$$\psi_\varepsilon(t) = \frac{A_\varepsilon}{(B+t)^\mu}\exp(-\varepsilon t) , \tag{E19}$$

whose Laplace transform can be written

$$\hat{\psi}_\varepsilon(s)=\frac{\hat{\psi}(s+\varepsilon)}{\hat{\psi}(\varepsilon)} . \tag{E20}$$

At lowest order in ε we obtain

$$\widehat{\Delta\psi}(s)\cong\varepsilon\left[\langle t\rangle\hat{\psi}(s)+\frac{d\hat{\psi}(s)}{ds}\right] . \tag{E21}$$

Making s tend to zero and using the asymptotic expression (C14) for $\hat{\psi}(s)$, we obtain

$$\begin{aligned}&\Delta\hat{\psi}(s)\cong-\varepsilon c(\mu-1)s^{\mu-2} ,\\ &\hat{\Psi}_0(s)\cong\langle t\rangle .\end{aligned} \tag{E22}$$

By replacing these expressions in (E9)–(E12) and using the inverse Laplace transform of $s^{\mu-5}$ [see (D9)], we obtain Eqs. (5.13)–(5.15). This way of determining the long-time behavior of the first moment adheres to the prescriptions of the method (i) illustrated in Sec. V.

To evaluate the response of the VM in the stationary case, we cannot apply this method, because if we adopted the expansion (E21) Eq. (1.2) would involve the second derivative of $\hat{\psi}(s)$ which diverges in the limiting case of s tending to zero. Therefore we apply method (ii) of Sec. V. We first make s tend to zero in (E19), and we obtain at lowest order in s

$$\Delta\hat{\psi}(s)\cong s\left[\frac{d\hat{\psi}(\varepsilon)/d\varepsilon}{\hat{\psi}(\varepsilon)}+\langle t\rangle\right] . \tag{E23}$$

Sending now ε to zero and using the asymptotic expression (C13) for $\hat{\psi}(\varepsilon)$ we get

$$\Delta\hat{\psi}(s)\cong s[-c(\mu-1)\varepsilon^{\mu-2}] , \tag{E24}$$

which gives

$$\frac{d\Delta\hat{\psi}}{ds}(s=0)=-c(\mu-1)\varepsilon^{\mu-2} . \tag{E25}$$

Replacing (E25) into (E13) we obtain the result (5.16). If we apply the same procedure to all the other theories, in both the stationary and nonstationary regimes, we recover the same results (5.16).

APPENDIX F

The effect of the first perturbation can be easily evaluated as follows. From the theory illustrated in Ref. [15] we derive that the parameter B of (2.3) is forced by the unperturbed map of Sec. III to get the value

$$B=2^{1/(\mu-1)}\frac{\mu-1}{a} . \tag{F1}$$

Notice that the unperturbed value of a is determined by the matching condition

$$\tilde{g}(\tfrac{1}{2})\equiv\tfrac{1}{2} , \tag{F2}$$

which sets

$$a=2^z . \tag{F3}$$

As mentioned in Sec. V the perturbation reduces the size of the left laminar region by the quantity p and leaves untouched the right laminar region. For numerical purposes it easier and more accurate to move the center of symmetry of the map (3.2) to the left by a quantity p in such a way as to make the right border of the left laminar region move to the left and the left border of the right laminar region to the left by the same quantity. Then from the matching condition

$$\tilde{g}_{\text{pert}}(\tfrac{1}{2}-p)=\tfrac{1}{2} \tag{F4}$$

we obtain

$$a_{\text{pert}}=\frac{(1-p)}{(\frac{1}{2}+p)^z} . \tag{F5}$$

Of course, for the perturbed value of B we get

$$B_{\text{pert}}=2^{1/(\mu-1)}\frac{\mu-1}{a_{\text{pert}}} . \tag{F6}$$

From this we can easily evaluate the parameter η, in terms of which the response to the geometrical perturbation is expressed in Sec. V. In the limiting case of weak perturbations ($p\ll 1$) we get

$$\eta=B_{\text{pert}}-B\approx(\tfrac{3}{2}\mu-\tfrac{1}{2})p . \tag{F7}$$

[1] N. G. van Kampen, *Stochastic Processes in Physics and Chemistry* (North-Holland, Amsterdam, 1981).

[2] H. Mori, H. Hata, T. Horita, and T. Kobayashi, Suppl. Prog. Theor. Phys. **99**, 1 (1989).

[3] E. Ott, *Chaos in Dynamical Systems* (Cambridge University Press, Cambridge, 1993).

[4] B. V. Chirikov, Prog. Rep. **52**, 265 (1979).

[5] G. Trefan, P. Grigolini, and B. J. West, Phys. Rev. A **45**, 1249 (1992); M. Bianucci, R. Mannella, X. Fan, P. Grigolini, and B. J. West, Phys. Rev. E **47**, 1510 (1993); M. Bianucci, L. Bonci, G. Trefan, B. J. West, and P. Grigolini, Phys. Lett. A **174**, 377 (1993).

[6] (a) T. Geisel, J. Nierwelberg, and A. Zacherl, Phys. Rev. Lett. **54**, 616 (1985); (b) M. F. Shlesinger and J. Klafter, *ibid.* **54**, 2551 (1985).

[7] A. Okubo, V. Andreaser, and J. Mitchell, Phys. Lett. **105A**, 169 (1984).

[8] *Polymer-Flow Interaction,* edited by Y. Rabin, AIP Conf. Proc. No. 137 (AIP, New York, 1985).

[9] R. Mauri and S. Hober, SIAM J. Appl. Math. **46**, 49 (1976).

[10] J. J. Prentis, J. Phys. A **18**, L833 (1985).

[11] L. F. Richardson, Proc. R. Soc. London Ser. A **110**, 709 (1926).

[12] E. W. Montroll and B. J. West, in *Fluctuation Phenomena,* 2nd ed., edited by E. W. Montroll and J. L. Lebowitz, Studies in Statistical Mechanics Vol. 7 (North-Holland, Amsterdam, 1987).

[13] E. W. Montroll and M. F. Shlesinger, in *From Stochastic to Hydrodynamics,* edited by J. L. Lebowitz and E. W. Montroll (North-Holland, Amsterdam, 1984).

[14] M. F. Shlesinger, B. J. West, and J. Klafter, Phys. Rev.

Lett. **58**, 1100 (1987).
[15] G. Zumofen and J. Klafter, Phys. Rev. E **47**, 851 (1993).
[16] G. Zumofen and J. Klafter, Physica A **196**, 102 (1993).
[17] G. Zumofen and J. Klafter, Physica D **69**, 436 (1993).
[18] J. W. Haus and K. W. Kehr, Phys. Rep. **150**, 263 (1987).
[19] M. F. Shlesinger, G. M. Zaslavski, and J. Klafter, Nature **363**, 31 (1993).
[20] R. Ishizaki, H. Hata, T. Horita, and H. Mori, Prog. Theor. Phys. **84**, 179 (1990); R. Ishizaki, T. Horita, T. Kobayashi, and H. Mori, *ibid.* **85**, 1013 (1991).
[21] D. K. Chaikovsky and G. M. Zaslavsky, Chaos **1**, 463 (1991).
[22] J. Klafter, G. Zumofen, and M. F. Shlesinger, Fractals **1**, 389 (1993); G. Zumofen and J. Klafter, Europhys. Lett. **25**, 565 (1994).
[23] R. Mannella, B. J. West, and P. Grigolini, Fractals **2**, 81 (1994).
[24] (a) P. Grigolini, *Quantum Mechanical Irreversibility and Measurement* (World Scientific, Singapore, 1993); (b) V. M. Kenkre, in *Exciton Dynamics in Molecular Crystals and Aggregates,* edited by V. M. Kenkre and P. Reineker, Springer Tracts in Modern Physics Vol. 94 (Springer, Berlin, 1982), p. 1.
[25] D. Bedeaux, K. Lakatos-Lindenberg, and K. E. Shuler, J. Math. Phys. **12**, 2116 (1971).
[26] V. M. Kenkre, E. W. Montroll, and M. F. Shlesinger, J. Stat. Phys. **9**, 45 (1973).
[27] V. Seshadri and B. J. West, Proc. Natl. Acad. Sci. U.S.A. **79**, 4051 (1982).
[28] R. Kubo, M. Toda, and N. Hashitsume, *Statistical Physics II, Nonequilibrium Statistical Mechanics,* 2nd ed. (Springer-Verlag, Berlin, 1991).
[29] X.-J. Wang, Phys. Rev. A **45**, 8407 (1992).
[30] G. Nicolis and C. Nicolis, Phys. Rev. A **38**, 427 (1988).
[31] T. Geisel, J. Heldstab, and H. Thomas, Z. Phys. B **55**, 165 (1984).
[32] S. Grossman, Z. Phys. B **57**, 77 (1984).
[33] R. Kubo, J. Phys. Soc. Jpn. **12**, 570 (1957).